EXCITED HYPERON OF MASS 1520 Mev*

Massimiliano Ferro-Luzzi,† Robert D. Tripp, and Mason B. Watson
Lawrence Radiation Laboratory, University of California, Berkeley, California
(Received December 13, 1961)

By investigating the K^-p interaction in the vicinity of 400 Mev/c, we have established the existence of an excited hyperon which is well described by the following properties:

mass: 1520 ± 3 Mev;

half-width: $\Gamma/2 = 8$ Mev;

isotopic spin: 0;

spin: 3/2;

parity: even with respect to K^-p ($D_{3/2}$);

branching ratios: $\bar{K}N:\Sigma\pi:\Lambda 2\pi = 3:5:1$.

In this study, the Lawrence Radiation Laboratory 15-in. hydrogen bubble chamber was placed in a separated K^- beam. The beam was separated at 760 Mev/c, and then degraded by a copper absorber placed in front of the chamber. The composition of the beam at 400 Mev/c was $K:\pi \simeq 7:1$. A total of 10 000 K^- interactions was measured and fitted.

Table I lists the five K^- momentum settings and the cross sections observed for each of the reactions. The only important bias correction is for small-angle K^-p scattering where a cutoff of $\cos\theta = 0.9$ (θ is the center-of-mass angle of the scattered K) was imposed and the total elastic cross section was obtained by extrapolating the differential cross section to 0 deg. The path length at each momentum was established from the number of τ decays. No significant ambiguity arose in the interpretation of the events, except for the case of the neutral-hyperon production. This involves disentangling $\Lambda\pi^0$, $\Sigma^0\pi^0$, and $\Lambda\pi^0\pi^0$ reactions ($\Sigma^0\pi^0\pi^0$ production may be neglected at these energies) among events in which a single Λ is observed associated with an incoming K^-. These events were selected on the basis of incoming K^- momentum as measured by curvature. Those whose curvature deviated by more than 1.5 standard deviations from the known beam momentum (as measured from τ decays) were not considered. Those accepted were averaged with their appropriate central beam momentum in order to obtain a better measure of the K^- momentum at the interaction point. This averaged momentum was then used to transform the decay-Λ kinetic energy into the center-of-mass system of the K^-p reaction and to compute the total missing mass

Table I. Cross sections (in mb) for the different K^- momenta (in Mev/c).

Reaction \ P_K	293 ± 42	350 ± 31	390 ± 30	434 ± 26	513 ± 20
K^-p	47.8 ± 4.1	33.5 ± 3.5	34.7 ± 3.2	32.8 ± 3.9	27.6 ± 3.7
$\bar{K}^0n$	8.0 ± 1.2	5.1 ± 1.1	8.8 ± 0.7	6.0 ± 1.2	3.6 ± 0.6
$\Sigma^+\pi^-$	13.1 ± 1.1	11.3 ± 1.6	13.5 ± 1.0	7.7 ± 1.2	7.3 ± 1.2
$\Sigma^-\pi^+$	9.7 ± 1.0	7.2 ± 1.0	8.0 ± 1.0	5.8 ± 0.9	4.7 ± 0.8
$\Sigma^0\pi^0$ [a]	5.2 ± 0.9	6.3 ± 1.4	6.7 ± 0.6	4.9 ± 1.3	1.4 ± 0.3
$\Lambda\pi^0$	5.2 ± 0.9	4.5 ± 1.0	3.1 ± 0.3	3.2 ± 0.7	1.9 ± 0.4
$\Lambda\pi^0\pi^0$ [b]	0.3 ± 0.2	1.9 ± 0.6	1.5 ± 0.2	0.8 ± 0.4	1.1 ± 0.3
$\Lambda\pi^+\pi^-$	0.15 ± 0.10	0.9 ± 0.3	1.6 ± 0.2	1.5 ± 0.4	2.0 ± 0.4
$\Sigma^0\pi^+\pi^-$	0 ± 0.02	0 ± 0.09	0.07 ± 0.06	0 ± 0.08	0.3 ± 0.15
$\Sigma^+\pi^-\pi^0$	0 ± 0.05	0.07 ± 0.07	0.21 ± 0.09	0.19 ± 0.10	0.20 ± 0.13
$\Sigma^-\pi^+\pi^0$	0.05 ± 0.05	0 ± 0.07	0.17 ± 0.08	0 ± 0.06	0.14 ± 0.10
Total	89.3 ± 4.6	69.3 ± 4.5	77.8 ± 3.6	62.8 ± 4.6	50.1 ± 4.1
$(\Sigma\pi)_0$	15.6 ± 2.7	18.9 ± 4.2	20.1 ± 1.8	14.7 ± 3.9	4.2 ± 0.9
$(\Sigma\pi)_1$	12.4 ± 2.3	5.9 ± 3.4	8.1 ± 1.9	3.7 ± 3.0	9.2 ± 1.6
$\pi\chi^2$	35.7	25.6	20.9	17.3	13.0

[a] Derived from $\sigma(\Sigma^0\pi^0) = \sigma(\Sigma^0\pi^0 + \Lambda\pi^0\pi^0) - \frac{1}{2}\sigma(\Lambda\pi^+\pi^-)$.

[b] Derived from phase-space considerations; as they stand they violate charge independence when compared with $\Lambda\pi^+\pi^-$.

required to conserve four-momentum. The $\Lambda\pi^0$ reactions (pure isotopic spin $1 = I_1$) appear as a Gaussian distribution centered around the square of the π^0 mass in an ideogram of the events plotted against missing mass squared. The widths of the observed distributions are related to the uncertainty of the measurements and are sufficiently narrow to allow a separation of these reactions from the I_0 part ($\Sigma^0\pi^0$ and $\Lambda\pi^0\pi^0$). The error introduced thereby is less than the statistical uncertainty. The further separation of the I_0 reactions into $\Sigma^0\pi^0$ (flat spectrum) and $\Lambda\pi^0\pi^0$ (whose spectrum presumably follows 3-body phase space like $\Lambda\pi^+\pi^-$) is more difficult since the spectra overlap considerably. However, for values of the missing mass larger than the maximum expected from a $\Sigma^0\pi^0$ reaction, the separation can be made, and the remainder of the $\Lambda\pi^0\pi^0$ spectrum is assumed to behave as phase space. Table I lists the $\Lambda\pi^0\pi^0$ cross sections obtained in this way. One can see that, at all momenta, $\sigma_{\Lambda\pi^0\pi^0} > \frac{1}{2}\sigma_{\Lambda\pi^+\pi^-}$. But $\sigma_{\Lambda\pi^0\pi^0}$ equals $\frac{1}{2}\sigma_{\Lambda\pi^+\pi^-}$ for $\Lambda\pi^+\pi^-$ production purely through I_0 and is less than that if any production takes place through I_1. We then infer that $\Lambda 2\pi$ production proceeds predominantly through I_0 at these energies,[1] and attribute the discrepancy to statistics and to a few poorly measured $\Sigma^0\pi^0$ events. To obtain the $\Sigma^0\pi^0$ cross section, we thus subtract $\frac{1}{2}\sigma_{\Lambda\pi^+\pi^-}$ from the I_0 neutral-hyperon production and take $\sigma_{\Lambda 2\pi} = \frac{3}{2}\sigma_{\Lambda\pi^+\pi^-}$.

The entries in Table I for $(\Sigma\pi)_0$ and $(\Sigma\pi)_1$ are obtained from the charge-independence relationships,

$$(\Sigma\pi)_0 = 3(\Sigma^0\pi^0)$$

and

$$(\Sigma\pi)_1 = (\Sigma^+\pi^-) + (\Sigma^-\pi^+) - 2(\Sigma^0\pi^0),$$

where the subscripts refer to the isotopic spin state.

It is seen from Table I that there is a considerable enhancement in $(\Sigma\pi)_0$, $\Lambda\pi^+\pi^-$, and $\bar{K}^0 n$ in the vicinity of 395 Mev/c, whereas $(\Sigma\pi)_1$ and $\Lambda\pi^0$ show no enhancement. We conclude that absorption takes place strongly in I_0 at this momentum. The resonant part of I_0 approaches $\pi\lambda\!\!\!^{-2}$, the maximum permissible for $J = \frac{3}{2}$. Since $\Lambda\pi^+\pi^-$ and $\bar{K}^0 n$ reactions are more precisely measured than those in other channels (typically $\delta P_K = \pm 7$ Mev/c and ± 5 Mev/c, respectively), one can study the momentum dependence of the cross section in more detail than is shown in Table I. We have merged all momenta and made an ideogram of the events vs momentum; from this we obtain the cross sections for $\Lambda\pi^+\pi^-$ and $\bar{K}^0 n$ shown in Figs. 1(a) and 1(b). These plots give us the mass and width of the excited state quoted above.

The total K^-p elastic cross section does not exhibit the enhancement at 395 Mev/c as well as the other channels because of the presence of a large nonresonant cross section. However, the differential K^-p cross section displays a striking behavior. Figure 2(a) is a plot of the coefficients A, B, and C in the least-squares fit of the differential K^-p cross section $d\sigma/d\Omega = (A + B\cos\theta + C\cos^2\theta)(\pi\lambda\!\!\!^{-2}/4\pi)$ mb/sr. It is seen that A dips at 395 Mev/c, whereas C is very large at the resonance and

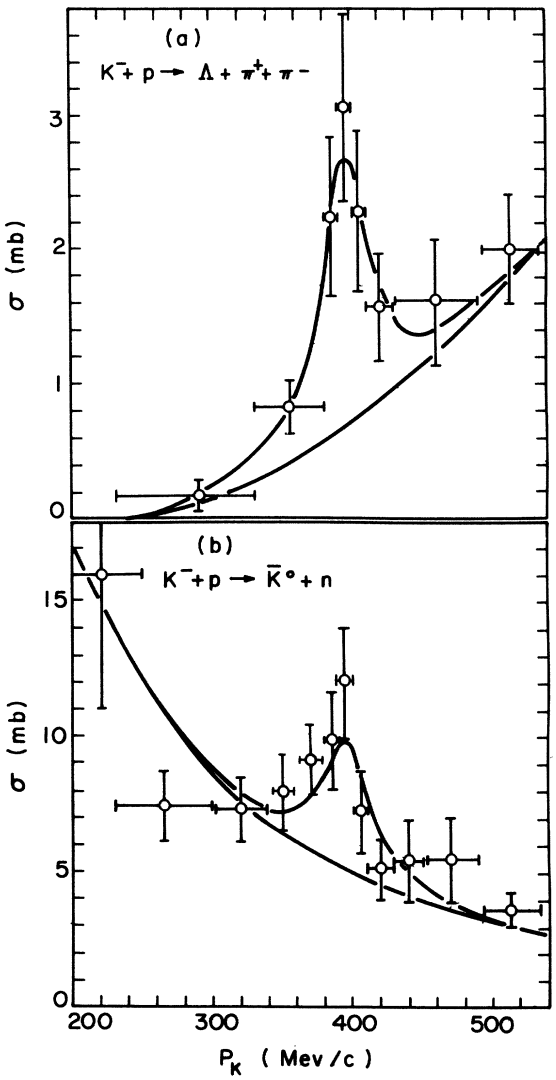

FIG. 1. Momentum dependence of the cross section for the reactions (a) $K^- + p \rightarrow \Lambda + \pi^+ + \pi^-$ and (b) $K^- + p \rightarrow \bar{K} + n$. The lower curves in (a) and (b) represent the presumed nonresonant backgrounds, while the upper curves contain in addition the superposed resonance.

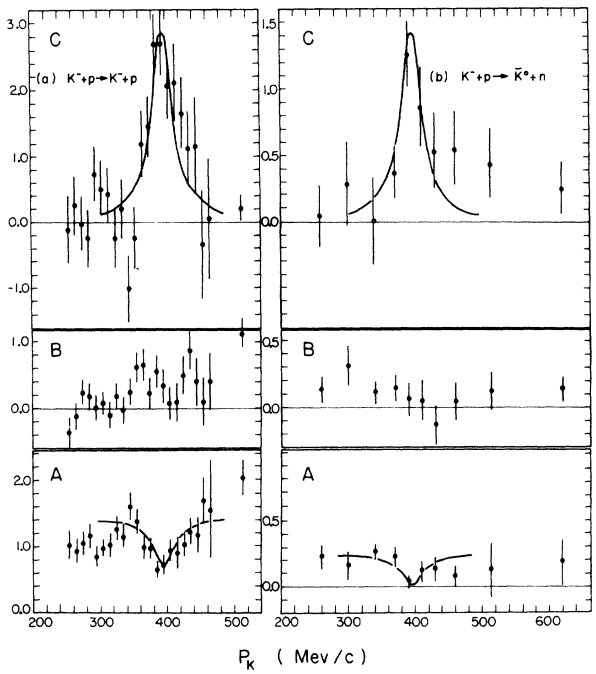

FIG. 2. Experimental points and calculated curves showing the momentum dependence of the coefficients of the angular distributions for the reactions (a) $K^-+p \rightarrow K^-+p$ and (b) $K^-+p \rightarrow \bar{K}^0+n$. The coefficients are dimensionless constants defined by $d\sigma/d\Omega = (A + B\cos\theta + C\cos^2\theta)(\pi\lambda^2/4\pi)$ mb/sr.

falls rapidly on both sides.[2] This suggests that the resonance interferes strongly with a state of the same parity. The nonzero value of B implies that a small monotonically rising amplitude of the opposite parity is also present. Below 250 Mev/c, all channels are consistent with a zero-effective-range S-wave analysis. We find the Humphrey-Ross (Solution I) S-wave scattering lengths to be in good agreement with this experiment,[3] apart from the resonance at 395 Mev/c and a small amount of P-wave scattering (<1 mb).

Figure 2(b) shows the quantities A, B, and C for charge-exchange scattering. Again the data fit the zero-effective-range solutions plus a resonant term at 395 Mev/c of the same parity.

The curves for A and C in Figs. 2(a) and 2(b) are constructed in the following manner. Since $K^-p = (I_0+I_1)/\sqrt{2}$ and $\bar{K}^0n = (I_0-I_1)/\sqrt{2}$, a resonance in a pure isotopic spin state yields equal enhancements in these channels. The nonresonant S-wave amplitudes are then obtained by subtracting a 5-mb resonant cross section from both K^-p and $\bar{K}^0n$ cross sections at 395 Mev/c, yielding $S_{\text{elastic}} = 1.2i$ and $S_{\text{charge exchange}} = 0.5i$ in accord with the corresponding nonresonant I_0 and I_1 absorption cross sections as well as the Humphrey-Ross solutions.[3] A resonant $D_{3/2}$ amplitude of the Breit-Wigner form $D = x/(\epsilon - i)$ is added, where $x = \Gamma_N/\Gamma$, $\epsilon = 2(E_\gamma - E)/\Gamma$, and $\Gamma = \Gamma_N + \Gamma_H$. Here Γ_N is the partial decay width of the excited hyperon into K^-p plus $\bar{K}^0n$, and Γ_H is the partial decay width into hyperon channels which may be further divided into $\Sigma\pi$ and $\Lambda 2\pi$. E is the total energy in the center-of-mass system, and $E_\gamma = 1520$ Mev is the resonant energy. The value $x = 0.35 \pm 0.05$ is obtained from the over-all best fit to the resonant bumps in the total cross sections for the various channels. It should be noted that the resonant and nonresonant amplitudes are essentially fixed by the total cross sections; hence the curves in Figs. 2(a) and 2(b) are predictions, not fits to the data. The angular distribution is of the form

$$\frac{d\sigma}{d\Omega} = \frac{\pi\lambda^2}{4\pi}\left[|P + (S+2D)\cos\theta|^2 + |S-D|^2\sin^2\theta\right],$$

where P is the $P_{1/2}$ amplitude, S is the S-wave amplitude, and D is the resonant $D_{3/2}$ amplitude.[4] From this expression it is seen that a relatively small D-wave amplitude is capable of producing the large $\cos^2\theta$ observed in the angular distribution without a concurrent large rise in the elastic cross section, in agreement with the experiment. The data are consistent with the resonant cross sections being the same in elastic and charge-exchange scattering, which shows that interference between the resonance and the I_1 amplitude of the same J and parity is small.

The alternative possibility of a $P_{3/2}$ resonance is beset with the following difficulties:

a. Assuming the isotropic part of the cross section to be largely S-wave, one would have to invoke a larger resonant amplitude in elastic than in charge-exchange scattering to account for the difference in C(elastic) and C(charge exchange). This would imply that the resonance is not in a pure isotopic spin state.

b. If one were to suppose that the S wave is small at the resonance and that $P_{1/2}$ and $P_{3/2}$ are the dominant amplitudes, then in some lower momentum region there must have been a transition from S to $P_{1/2}$, resulting in a large $\cos\theta$ term in the transition region. There is no evidence for a large B anywhere below 400 Mev/c in Figs. 2(a) and 2(b). Since absorptive processes are strong, the scattering amplitudes are largely imaginary; thus the possibility is extremely remote that S- and P-wave amplitudes are orthogonal throughout this region and therefore do not

yield a large B term.[5] Moreover, the momentum dependence of the nonresonant parts of the $\bar{K}N$ cross sections is consistent with S waves and is not that to be expected for P waves.

The coefficients B in Figs. 2(a) and 2(b) suggest a uniformly increasing P-wave cross section. If the P-wave amplitude is taken to be imaginary (purely absorptive), its magnitude is in satisfactory agreement with the amount of absorption from this state required by the hyperon angular distributions and polarizations.

The resonant cross section for $\Sigma\pi$ plus $\Lambda 2\pi$ production is $\pi\lambda^2[4x(1-x)/(\epsilon^2+1)]$. Since x is less than $\frac{1}{2}$, the excited hyperon is coupled more strongly to the pion-hyperon systems than it is to the K-meson–nucleon system. The branching ratios are $\bar{K}N:\Sigma\pi:\Lambda 2\pi = 3:5:1$, where the symbols mean the sum of rates into all charge states. The angular distributions and polarization in hyperon production are in good agreement with the picture presented above. A discussion of $\Sigma\pi$ angular distributions and polarizations and their relationship to the Σ parity will be presented in the near future.

We thank the other members of this collaborative experiment, P. L. Bastien, J. P. Berge, O. I. Dahl, J. Kirz, D. H. Miller, J. J. Murray, and A. H. Rosenfeld, for their efforts in obtaining the data. We also thank Professor L. W. Alvarez for his support and encouragement. The help from our scanners, D. J. Church, C. Dudley, M. F. Kelly, C. Owens, and R. Tye, in finding and analyzing the events is gratefully acknowledged.

---

*Work sponsored by the U. S. Atomic Energy Commission.

†National Academy of Sciences Fellow.

[1]A Dalitz plot of T_{π^+} vs T_{π^-} of $\pi^+\pi^-$ shows no statistically significant deviation from uniformity. An admixture of I_0 and I_1 would in general produce an asymmetry in the Dalitz plot about the line $T_{\pi^+} = T_{\pi^-}$. There is no clear evidence for the production of $Y_1^* + \pi$ (threshold = 1520 Mev). Whether the coincidence of this threshold with the excited-hyperon mass is fortuitous is beyond the scope of this paper.

[2]The presence of a large $\cos^2\theta$ term at 400 Mev/c was observed in earlier experiments. See L. W. Alvarez, in Ninth International Annual Conference on High-Energy Physics, Kiev, 1959 [Academy of Sciences (UPAP), Moscow, Russia, 1960], and Lawrence Radiation Laboratory Report UCRL-9354, 1960 (unpublished); and P. Nordin, Phys. Rev. 123, 2168 (1961). R. H. Capps, Phys. Rev. Letters 6, 375 (1961), has conjectured that this arises from a $D_{3/2}$ interaction.

[3]W. E. Humphrey [Lawrence Radiation Laboratory Report UCRL-9752, 1961 (unpublished)] and R. R. Ross [Lawrence Radiation Laboratory Report UCRL-9749, 1961 (unpublished)] have analyzed the low-energy K^-p data and find two solutions consistent with this data. The preferred one (also favored by other experiments) gives for the I_0 and I_1 scattering lengths (in fermis) $A_0 = (-0.22 \pm 1.07) + i(2.742 \pm 0.31)$, and $A_1 = (+0.019 \pm 0.33) + i(0.384 \pm 0.075)$. These scattering lengths yield the following values of the S-wave amplitudes for elastic and charge-exchange scattering at 395 Mev/c: $S_{\text{elastic}} = (0 \pm 0.2) + (1.1 \pm 0.1)i$; $S_{\text{charge exchange}} = (0 \pm 0.2) + (0.5 \pm 0.1)i$. Deviations from the momentum dependence of the elastic and charge-exchange cross sections predicted by the above values of A_0 and A_1 do occur at 513 Mev/c. This could be due to P-wave scattering or to the onset of effective-range corrections to the S waves, or to both.

[4]This form can be obtained immediately from the familiar S, $P_{1/2}$, and $P_{3/2}$ expansion by a Minami transformation: $S \rightarrow P_{1/2}$, $P_{1/2} \rightarrow S$, $P_{3/2} \rightarrow D$. We disregard $P_{3/2}$ in the transformed expression, since in none of the many angular distributions do we see any evidence for $\cos^3\theta$ expected from a $P_{3/2}$-$D_{3/2}$ interference. Nor do we find any need for $\cos^4\theta$ terms, so that the angular momentum of the resonance is very unlikely to be higher than $\frac{3}{2}$.

[5]Comparison between the forward-scattering amplitude $f(0)$ and $\mathrm{Im}f(0)$ obtained from the optical theory shows $\mathrm{Re}f(0)$ to be consistent with zero, in agreement with this conclusion.